Int. J. Electrochem. Sci., 12 **(2017)** 10674 – 10686, doi: 10.20964/2017.11.56

International Journal of
ELECTROCHEMICAL
SCIENCE
www.electrochemsci.org

Electrochemical and Mechanical Properties of Sodium-Ion Conducting Cross-Linked Polymer Gel Electrolyte

Yuan Xue[1,*], *Xiang Li*[2], *David J. Quesnel*[1]

[1] Materials Science Program and Mechanical Engineering Department, University of Rochester, Rochester NY 14627, USA,
[2] Microsystems Engineering Program and Chemical Engineering Department, Rochester Institute of Technology, Rochester, NY 14623, USA,
[*]E-mail: yxue4@ur.rochester.edu

Received: 27 July 2017 / *Accepted:* 6 September 2017 / *Published:* 12 October 2017

The free radical polymerization of cross-linked poly(methyl methacrylate) (PMMA) polymer gel electrolyte (PGE) for sodium-ion transport exhibits high ionic conductivity, good mechanical property and low cost. Appropriate amounts of sodium hexafluorophosphate ($NaPF_6$) were arbitrarily added into cross-linked PGEs in order to decrease the crystallinity of the polymer and to provide more charge carriers to facilitate ionic conductivity. The Shore A durometer test revealed that the $NaPF_6$ addition also enhanced the hardness of the cross-linked PGEs. The highest ionic conductivity obtained was 1.33×10^{-3} S cm^{-1} for the cross-linked PGE with 20 wt.% $NaPF_6$. Activation energies calculated based on Arrhenius behavior for cross-linked PGEs with 10 wt.%, 20 wt.% and 30 wt.% $NaPF_6$ additions were 0.13, 0.10 and 0.16 eV, respectively. The electrochemical window was from -2.5 V to 2.5 V and the transference numbers was ranging from 0.9 to 0.96. This work demonstrates that the adoption of cross-linking technique and $NaPF_6$ opens the door to facile synthesis of sodium ion conductive PGEs, in which the mechanical property and electrochemical behavior are easy to be tailored by simply tuning $NaPF_6$ additives. The enhancement of hardness and ionic conductivity of cross-linked PGEs enable their potential applications in advanced energy storage systems.

Keywords: Polymer gel electrolyte; Electrochemistry; Cross-linked poly(methyl methacrylate); Sodium hexafluorophosphate; Sodium ion conducting

1. INTRODUCTION

The advancement of safe and reliable secondary batteries based on lithium and sodium has been limited, in part, by the electrolyte. The electrolyte plays a critical role in the adoption of secondary batteries as a renewable energy source since it directly influences the batteries' efficiency, cost, lifetime, and safety [1-3]. Solid polymer electrolytes, which were first reported in the 1970s, have been intensively investigated due to their attractive capability of transporting ions between electrodes [4]. For example, the ionic conductivity of poly(ethylene oxide) (PEO) complexed with alkali metal salts was shown by Wright in 1973 to be 10^{-8} S cm^{-1} with 200-300 useful life cycles in a lithium-ion battery [4]. This finding triggered hundreds of papers dealing with the fabrication and modification of solid polymer electrolytes. Sreekanth studied sodium-ion conducting polymer electrolytes based on PEO doped with different sodium nitrate ($NaNO_3$) compositions [5]; the highest ionic conductivity obtained was 10^{-6} S cm^{-1} at room temperature with 30% $NaNO_3$ addition. However, the ionic conductivity of solid polymer electrolyte was dramatically limited at its early stages. Additionally, poor dimensional stability created another drawback of solid polymer electrolytes [6]. To overcome the above disadvantages, polymer gel electrolytes (PGEs) have been introduced. A PGE is a solid system consisting of a polymer matrix, organic solvents, and salts [7]. In comparison to solid polymer electrolytes, PGEs are a more appealing choice as they combine high ionic conductivity, low cost, improved safety, and ease of fabrication into desired shapes and sizes [8-10]. Nevertheless, it should be pointed out that even with immense efforts directing towards PGEs, the conductivity of PGEs is still restrained because of the organic solvent evaporation that reduces the volume of the electrolyte [11,12]. A decrease in the electrolyte volume causes a decrease of the electrolyte/electrode contact area and disrupts the path for ionic conductivity. The poor mechanical strength also limits the application of PGEs for the use of large capacity battery modules [13]. Quartarone had found a small amount of volume reduction in PGE membranes which were made of on poly(methyl methacrylate) (PMMA), EC/DMC organic liquid mixtures and lithium salt [14]. They stated that this phenomenon was possibly caused by the onset of phase separation with aging. A possible solution to this issue is incorporating excess solvent in the fabrication of the PGE for maintaining better stability of electrolyte and electrode. Cross-linked polymers are another alternative to solving the performance decay of PGEs. Cross-linked polymers are formed by bonding between neighboring monomers which are networked by short side chains making them stronger and more stable. This idea may arise from the assumption that the branched chains that are chemically cross-linked will improve the dimensional stability due to the enhanced chain entanglements [15].

In the present study, we employ PMMA to build up a matrix, which is a highly affine linear-chained polymer where the side functional group $-COOCH_3-$ is compatible with plasticizers, and enables the methyl methacrylate structural units to trap and efficiently store organic liquids. The monomer methyl methacrylate (MMA) will be cross-linked with the presence of a cross-linker, and then free radically polymerized with an initiator under nitrogen to form cross-linked PMMA. Sodium hexafluorophosphate ($NaPF_6$) was chosen as a charge carrier provider because of the weak interaction between non-coordinating anions PF_6^- and the cation. The large molecular weight of PF_6^- and small solvation energy indicate that when $NaPF_6$ is added into the solvent [16], it is able to undergo a greater degree of dissociation, thus releasing more sodium ions to provide more charge carriers while decreasing aggregation. Besides holding good ion transfer ability, mechanical property of electrolyte is one of the most concerning issues that needs to be evaluated especially for long term operation. However, by now, the mechanical property study of PGEs is still rudimentary. The present work studied the mechanical property of cross-linked PGEs in terms of hardness immediately upon their successful synthesis, and the results showed that the hardness of cross-linked PGEs is strengthened and tailorable with $NaPF_6$ additives. The organic liquids PC/EC are used to soften the polymer backbones and increase their segmental motions. $NaPF_6$, species solvated in organic liquids, are accommodated within the three-dimensional polymeric networks of cross-linked PGEs through surface tension [17]. Hence, the ionic conductivity of cross-linked PGEs can be enhanced by $NaPF_6$ solvated in organic liquids and further immobilized inside the polymer framework. The main goal of the present research is to develop a cross-linked PMMA based PGE with high ionic conductivity along with good mechanical stability for overcoming the organic solvent evaporation problem. A combination of various electrochemical and mechanical techniques in terms of electrochemical impedance spectroscopy, cyclic voltammetry, transference number measurements, and Shore A durometer hardness testing were employed in this study to characterize the cross-linked PGE.

2. EXPERIMENTAL

2.1 Materials

Cross-linked polymer gel electrolyte (PGE) membranes were prepared by a free radical polymerization technique. Methyl methacrylate (MMA), 99%, stabilized, benzoyl peroxide (BPO), propylene carbonate (PC), ethylene carbonate (EC) and sodium hexafluorophosphate ($NaPF_6$) were purchased from Alfa Aesar (Ward Hill, MA). Neopentyl glycol dimethacrylate (NPG) obtained from TCI America (Portland, OR) was used as the cross-linker. The ionic liquid solution and monomer were prepared separately in two beakers at room temperature. Cross-linking agent NPG, 0.036 ml was added into 3.23 ml (3 grams) of MMA under nitrogen protection. Then organic solvent was prepared by mixing PC and EC (solid at room temperature) in a weight ratio of 1:2 (1.5 grams of PC and 3 grams of EC). The amount of sodium hexafluorophosphate ($NaPF_6$) that was added into PC/EC mixture was calculated as a fraction of the total weight (including the weight of monomer, organic liquid solution PC/EC and $NaPF_6$). Target salt masses ranged from 0 to 30 wt.%. The monomer and organic ionic liquid solution were mixed in a reaction vessel (battery jar) with a radius of 2.5 cm under nitrogen environment at room temperature. Benzoyl peroxide (BPO) with appropriate amount (0.1–0.15% of the monomer mixture by weight) was added to the solution. The solution was kept stirring thoroughly for 30 minutes under nitrogen. Then the mixture was placed in water bath at $75 \pm 1\ ^{\circ}C$ for four hours to fulfil polymerization. After the solution solidified, a cross-linked polymer gel electrolyte membrane based on PMMA was formed. The PMMA-PGE was removed from the reaction vessel and placed in the fume hood over night for further drying. Once the residual monomer evaporated, free-standing membranes with thickness from 0.22 cm to 0.26 cm were trimmed into a radius of 1.5 cm for further characterization.

2.2 Methods

The morphologies of cross-linked PGE samples were observed by scanning electron microscopy (SEM) using a TESCAN MIRA3 system of the Center for Imaging Science at the

Rochester Institute of Technology. The hardness of the cross-linked PGEs was measured by Shore A Durometer scale digital hardness tester with a range of 0100 HA and 0.5 HA accuracy. Three identical cross-linked PGEs with the same composition were stacked together for total thickness of 0.67 cm, sufficient to enable durometer indentations. Ten indentations were applied to every sample. The cross-linked PGE membrane was sandwiched by two circular aluminum electrodes (radius: 1.5 cm) on both sides for electrochemical tests. The aluminum plates were used as ion-blocking electrodes. The electrochemistry studies of the samples were carried out using a Gamry Reference-600. The ionic conductivity of the cross-linked PGE was studied with Electrochemical Impedance Spectroscopy (EIS) in the frequency range from 100 Hz to 1 MHz AC voltage. The electrochemical stability of the sample was evaluated using cyclic voltammetry from -4 V to 4 V and a scan rate of 50 mV/s. The set-up of aluminum/cross-linked PGE/carbon was built for ionic transference number measurement through d.c. polarization method with a constant voltage of 1 V. The polarization current was recorded as a function of time.

3. RESULTS AND DISCUSSION

3.1 Morphology

A typical cross-linked PGE sample with 5 wt.% $NaPF_6$ synthesized by free radical polymerization is shown in Fig. 1(a), suggesting the cross-linked PGE is homogeneous, free-standing, flexible, and transparent.

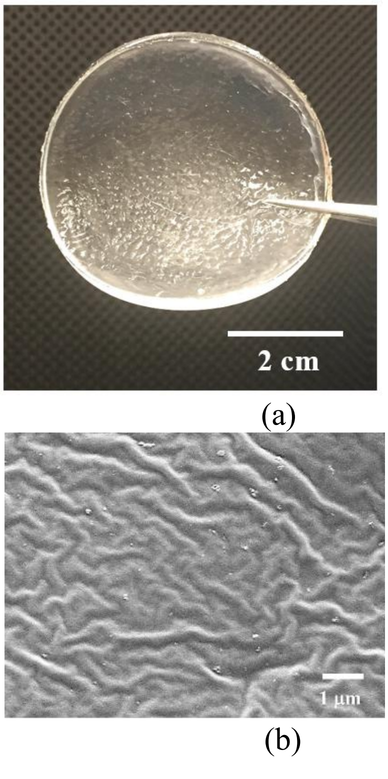

(a)

(b)

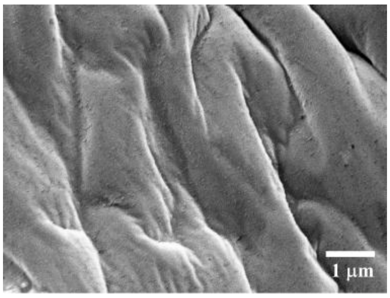

(c)

Figure 1. Picture of cross-linked PGE with 5 wt.% $NaPF_6$ (a), SEM micrograph of cross-linked PGE without salt with wrinkled texture (b), and SEM micrograph of cross-linked PGE with 5 wt.% $NaPF_6$ with increased wrinkle width (c).

The thickness of this sample was 0.23 cm and the salt $NaPF_6$ is evenly distributed in the cross-linked PGE without any salt aggregation as assessed by the SEM images. SEM inspection showed detailed patterns of the cross-linked PGE without $NaPF_6$ (Fig. 1b) and with 5 wt.% $NaPF_6$ (Fig. 1c). The wrinkled texture, which is found in both Fig. 1(b) and 1(c), was probably generated because the sample differs in surface tension due to the stress fields and dimensional changes introduced by polymerization.

The wavy wrinkles can be recognized as accommodation of organic liquids and salt additives for creating the continuous paths for ion transport. SEM also confirmed that the wrinkle width expanded from 0.2 ~ 0.3 μm in Fig. 1(b) to 2 μm after 5 wt.% $NaPF_6$ was added, Fig. 1(c).

3.2 Mechanical property

Upon successful synthesis of cross-linked PGE, its mechanical property is examined in terms of hardness. The cross-linked PGE is a very soft material, which possesses elasticity similar to that of a gel shoe insole with the hardness value of 30 in Shore OO. The hardness of cross-linked PGEs with various $NaPF_6$ additives were measured by Shore A durometer and plotted as a function of the $NaPF_6$ concentration in Fig. 2. Reading the hardness values for cross-linked PGEs and comparing them with the Shore Durometer standard chart, one could infer that the cross-linked PGEs exhibit higher hardness than that of a typical rubber band and the hardness value is located within the medium soft range, somewhat analogous to an eraser whose hardness value is about 40 in Shore A. The dimensional stability of cross-linked PGE is able to be improved due to chain tangling caused by cross-linking. Additionally, from Fig. 2, the hardness increases proportionally with increase in the $NaPF_6$ concentration. This is due to the higher concentration of $NaPF_6$ introduced more salts per unit volume, which establishes stronger interactions between the polymer matrix and conducting medium. The stronger interactions generate more resistance that repels the deformation in Shore A durometer tests and further favor a more mechanical robust cross-linked PGE.

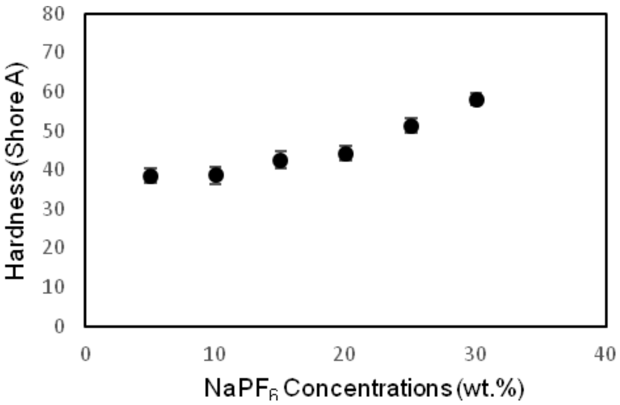

Figure 2. Hardness of cross-linked PGEs based on Shore A durometer measurements as a function of salt concentration. Error bars represent 10 readings for each concentration.

3.3 Ionic Conductivity

The hardness test has proved that the mechanical property of cross-linked PGE is substantially improved by $NaPF_6$ additives. An important electrochemical factor of the cross-linked PGE is the ability to transport ions between electrodes, which is also called ionic conductivity. It is noteworthy that the $NaPF_6$ not only strengthens the structure of cross-linked PGE, but also fulfil the ionic conductivity by playing the role of charge carrier provider. Thus, theoretically, more $NaPF_6$ is favorable for both mechanical robust and ion transfer capability. Nevertheless, it needs to be pointed out that over doping $NaPF_6$ would introduce too much undissolved $NaPF_6$ in organic liquid, which occupies the ion transfer pathway so that hinders ion movement.

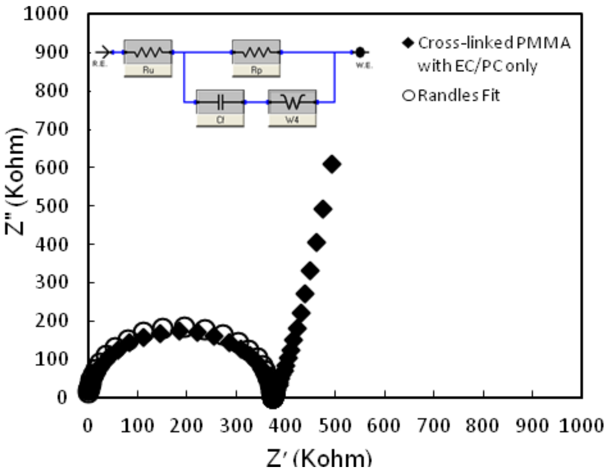

Figure 3. Nyquist plot of the cross-linked PGE without salt (in black diamond), and fitted by the Randles model (in white circle); in the equivalent circuit (the inset), R_u is the bulk resistance, R_p is the polarization resistance, C_f is the double layer capacitance and W_4 is the Warburg resistance.

Given above consideration, it is necessary to investigate the $NaPF_6$ concentration dependence of ionic conductivity in order to optimize the $NaPF_6$ additives for compromising the mechanical strength and ionic conductivity. The experimental results confirmed that the $NaPF_6$ has significant effect on the ionic conductivity of cross-linked PGE. EIS is a powerful tool to characterize electrochemical activity of cross-linked PGEs [18]. A Nyquist plot of the cross-linked PGE without salt is given in Fig. 3, which features a semicircle in the high frequency region and a spike in the low frequency region. This characteristic EIS spectra suggests the cross-linked PGE is a typical ion conductor and this finding agrees with literature reports [19,20]. The semicircle is well fitted by the Randles model shown in the inset of Fig. 3.

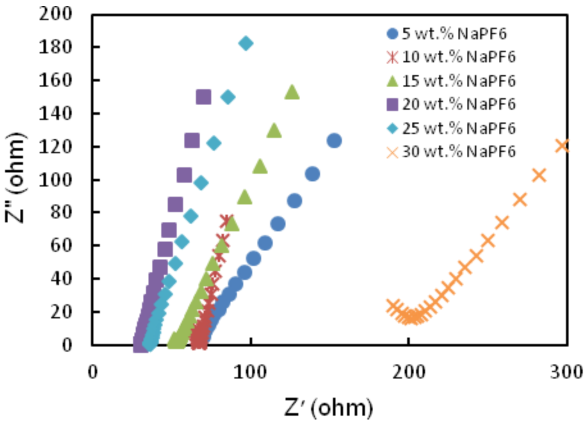

Figure 4. Nyquist plots of cross-linked PGEs with various $NaPF_6$ concentrations from 5 wt.% to 30 wt.% (the blue circle: PGE with 5 wt.% $NaPF_6$; red star: PGE with 10 wt.% $NaPF_6$; green triangle: PGE with 15 wt.% $NaPF_6$; purple square: 20 wt.% $NaPF_6$; blue diamond: PGE with 25 wt.% $NaPF_6$; orange x: PGE with 30 wt.% $NaPF_6$).

Table 1. The ionic conductivity of cross-linked PGE with various $NaPF_6$ concentrations.

Weight Percentages of $NaPF_6$ in PGE (w.t.%)	Ionic Conductivity σ (S cm^{-1})
0	8.15×10^{-8}
5	4.73×10^{-4}
10	5.09×10^{-4}
15	6.82×10^{-4}
20	1.33×10^{-3}
25	1.05×10^{-3}
30	2.25×10^{-4}

The bulk resistance R_u and polarization resistance R_p are extracted from the intercept on the real axis (Z') in high frequency and middle frequency region, respectively. The spike is referred to as the Warburg resistance (W_4) due to the ion diffusion and heterogeneous surface of the electrode [21,22]. The resistance for cross-linked PGE without salt is obtained from Fig. 3 as 3.76×10^5 ohms. The ionic conductivity for the cross-linked PGE can be calculated from the following Eq. [23]:

$$\sigma = \lambda/(R_b \times A) \qquad (1)$$

where λ is the membrane thickness in cm, R_b is the resistance of the cross-linked PGE in ohms from EIS data, and A is the surface area of the electrode, in this case is 7 cm^2. The ionic conductivity of the cross-linked PGE without salt is 8.15×10^{-8} S cm^{-1}. Cross-linked PGEs with various $NaPF_6$ additions were characterized by EIS sequentially with the Nyquist plots displayed in Fig. 4. Based on Eq. 1, the ionic conductivities associated to the different $NaPF_6$ concentrations are listed in Table 1.

The ionic conductivity of various cross-linked PGEs samples is summarized in Fig. 5. It is apparent that not as same as hardness, which is increased with $NaPF_6$ increment, a trend of the ionic conductivity of cross-linked PGEs is observed to increase proportionally with the addition of $NaPF_6$ from 0 to 20 wt.%, then to decrease with continuous salt addition. The ionic conductivity of the cross-linked PGE with 5 wt.% $NaPF_6$ has increased four orders of magnitude compared to the cross-linked PGE without $NaPF_6$. This phenomenon is likely due to the increases in ion concentration in the organic liquid with more ions providing more charge carriers which enhance ion transport, as well as the amorphousness increase by the increasing salt concentration [24]. The peak ionic conductivity of 1.33×10^{-3} S cm^{-1} is obtained when the salt concentration reaches 20 wt.% of the cross-linked PGE. The ionic conductivity reported in this work is comparable with other PGEs doped with lithium, sodium or aluminum ionic liquids [25-28]. For example, in Yang and coworkers' research, they observed the ionic conductivity of 6×10^{-4} S cm^{-1} of the sodium ion conducting gel polymer electrolyte[29]. Comparing to Yang's work, the ionic conductivity of PGE in present work is 50% higher. Noting that segmental motion of the polymer chains in the elastomeric phase is able to enhance ion transport, in the present study, we developed a cross-linked PGE, whose structure incorporated a highly flexible backbone and amorphous phase, for the purpose of improving the ionic conductivity of sodium-ion conductors. When additional salt species were added beyond the maximum conductivity at 20 wt.%, a sharp decline is observed for the cross-linked PGE. This may be caused by the limited solubility of $NaPF_6$ in the organic solvents, PC and EC so that the crystal salt occupied the free volume thus hinder the ion transportation. The other reason for the ionic conductivity decrease with increased addition of salt may be that the neutral ion aggregates formed by cations which will not be able be counted as charge carrier [24,30].

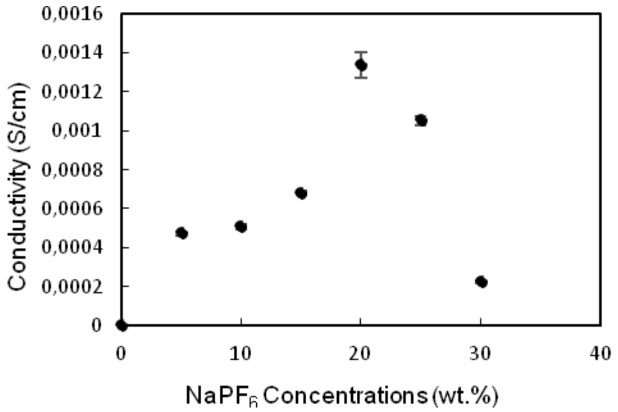

Figure 5. Ionic conductivities of cross-linked PGEs with $NaPF_6$ concentrations at 0 wt.%, 5 wt.%, 10 wt.%, 15 wt.%, 20 wt.%, 25 wt.% and 30 wt.%. All the values of ionic conductivity with error bars were calculated from 5 tests.

The ionic conductivity of cross-linked PGEs with elevated temperature from 20 °C to 60 °C was studied and the temperature dependence of ionic conductivity of various samples was plotted in Fig. 6, in which the temperature dependence behavior can be described by the Arrhenius equation [31]:

$$\sigma = \sigma_0\, exp\ (-E_a / k\mathrm{T}) \qquad (2)$$

where σ_0 is the conductivity pre-exponential factor, E_a is activation energy, k is the Boltzmann constant, and σ is the conductivity. A linear relationship between the logarithm of the ionic conductivity and the reciprocal of the temperature is inferred from Fig. 6, a behavior similar to that of isotropic ionic liquids [18]. The ionic conductivity values of cross-linked PGEs associated with 5 wt.%, 10 wt.%, and 20 wt.% increased with temperature. This is due to the fact that ions are thermally activated by the elevated temperature which enhances ion transfer within the polymer matrix by providing more free volume for polymer chain movements [32]. Furthermore, the elevated temperature promotes the expansion of polymer matrix which provides larger free volume for ions transportation [33]. Activation energy is a quantitative approach to understand the mechanism for the movement of ions through the cross-linked PGEs along the continuous paths created by ionic liquids. The activation energy E_a of cross-linked PGEs is calculated from Fig. 6. The E_a for cross-linked PGEs with 10 wt.%, 20 wt.%, and 30 wt.% $NaPF_6$ are 0.13 eV, 0.10 eV, and 0.16 eV, respectively. This explains the energy needed and how difficult for an ion to hop or jump from its normal position to a neighboring equivalent site [34]. During battery operation, the lower the activation energy needed for ion motion, the higher the mobility of ions is. Hence, with $NaPF_6$ increasing from 10 wt.% to 20 wt.%, the activation energy decreases, which indicates that the movement of ions is facilitated, and as a result, higher ionic conductivity is obtained which is in good agreement with the ionic conductivity of cross-linked PGEs with different $NaPF_6$ concentrations in our present work. Higher concentration of $NaPF_6$ in the cross-linked PGE creates more neighboring equivalent sites and shortens the migration distance for ionic movement, lowering the activation energy and enhancing the ionic conductivity. Moreover, $NaPF_6$ addition will decrease the crystallinity of the polymer matrix resulting in lower activation energy. The activation energy of cross-linked PGEs in present study is comparable with other peer researchers. For instance, Cao and coworkers had synthesized the perluorinated sulfonic membrane in the Na-form (PFSA-Na) swollen with nonaqueous solvents EC-PC that could be used as electrolyte. They had obtained the activation energy of PFSA-Na as 0.161 eV [35].

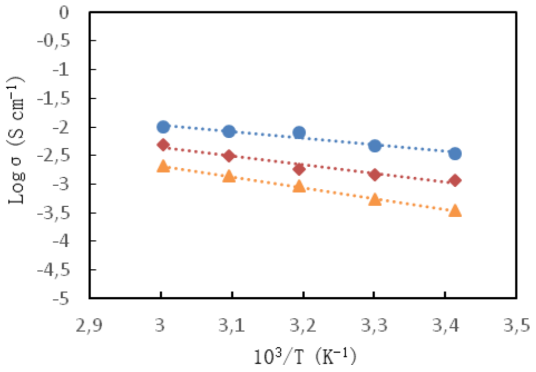

Figure 6. Temperature dependence of ionic conductivity for cross-linked PGEs with 10 wt% $NaPF_6$ (in red diamond), 20 wt.% NaPF6 (in blue circle) and 30 wt.% $NaPF_6$ (in orange triangle).

3.4 Electrochemical Window

Cyclic voltammetry was chosen to study the electrochemical stability of the sodium ion conducting cross-linked PGEs. The electrochemical window defines the potential range that an electrolyte is electrochemically stable. Water for example has a 1.23 V electrochemical window between the reduction of hydrogen to form H_2 gas and the oxidation of water to liberate O_2 gas. This is known as the stability range for water. In batteries, the chemical electron transfer reactions occur at specific potentials that must reside within the stability range of the electrolyte, limiting the potential differences realizable in a particular electrolyte. Thus, a wide chemical window is desired to ensure stability in practical operation of batteries in order that the electrolyte itself does not undergo oxidations or reductions. The cyclic voltammogram in Fig. 7 reveals that the electrochemical window for the cross-linked PGE with 20 wt.% $NaPF_6$ is valid from -2.5 V to 2.5 V, over which no reduction or oxidation peaks are obtained. The results of the electrochemical window are the same as Kumar and coworker's work of the nano-composite PMMA based GPEs with $NaClO_4$ dissolved in EC-PC, which enabled the potential window from -2.5 V to 2.5 V [36,17]. Therefore, the electrochemical window of our cross-linked PMMA PGE is 5 V, which is higher than 4.5 V electrochemical window observed for the PFSA-Na membrane in Cao's work [35]. From these studies, we determined that the cross-linked electrolyte is suitable for battery systems where electron transfer reactions are within a working electrochemical window of 5 V.

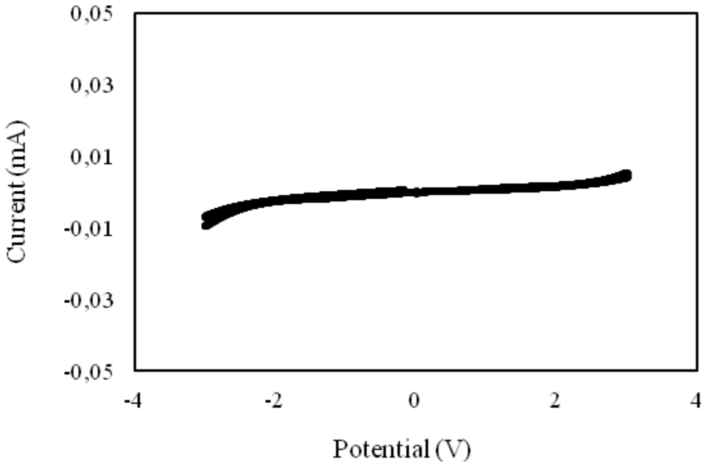

Figure 7. Electrochemical window plot for cross-linked PGE with 20 wt.% $NaPF_6$ measured by cyclic voltammetry with potential varied from -3 V to 3 V. No oxidations or reductions take place in the electrolyte indicating its stability.

3.5 Transference Number

The transference number measurements for cross-linked PGEs with various concentrations of $NaPF_6$ were carried out using d.c. polarization techniques. The sample was sandwiched by an aluminum electrode and a carbon electrode on each side. Then, a constant d.c. voltage of 1 V was applied across the cell and the resulting current was recorded as a function of time. Transference numbers of cross-linked PGEs with 5 - 20 wt.% $NaPF_6$ are shown in Fig. 8. Once the potential started, the ions became increasingly polarized, and the current could be harvested from the external circuit, eventually falling to zero. As the potential is continuously applied on the sample, the current drops dramatically as a result of the ions losing their mobility. The transference number values, denoted as t_{ion}, can be calculated based on the following equation [37,38]:

$$t_{ion} = (I_I - I_f) / I_I \qquad (3)$$

where I_I is the initial current during polarization and I_f is the final current. The transference numbers for cross-linked PGEs with $NaPF_6$ are calculated and listed in Table 2. From Table 2, the transference numbers are found in the range of 0.90~0.96, which is similar to Bhargav's report, in which the total ionic transference number was obtained from 0.929 to 0.948 for electrolytes implying that the conductivity of cross-linked PGEs is predominantly a consequence of ionic motions instead of being due to electrons [5] [39].

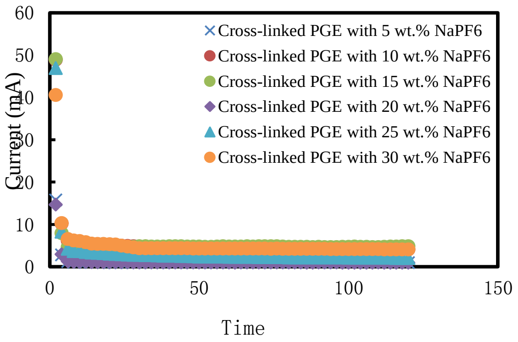

Figure 8. D.C. polarization curves of cross-linked PGEs with $NaPF_6$ concentrations ranging from 5 wt.% to 30 wt.% (the blue x: PGE with 5 wt.% $NaPF_6$; red circle: PGE with 10 wt.% $NaPF_6$; green circle: PGE with 15 wt.% $NaPF_6$; purple diamond: 20 wt.% $NaPF_6$; blue triangle: PGE with 25 wt.% $NaPF_6$; orange circle: PGE with 30 wt.% $NaPF_6$).

Table 2. Transference numbers of cross-linked PGEs for various salt concentrations

$NaPF_6$ (wt.%) in Cross-linked PGE	Transference number
5	0.938
10	0.916
15	0.911
20	0.932
25	0.956
30	0.900

4. CONCLUSIONS

PMMA-based cross-linked PGEs with various $NaPF_6$ concentrations associated in EC/PC organic liquids were polymerized by the free radical approach and were characterized using SEM, Shore A durometer, EIS, CV, and current leakage techniques. The cross-linked PGE exhibits good mechanical properties with high ionic conductivity and low cost. The cross-linked PGEs are flexible and free standing upon successful fabrication. Morphology investigation carried out by SEM that revealed continuous paths created by plasticizers in the polymer framework favoring ion transportation. The addition of sodium ions dissociated within organic solvents increases the ionic conductivity of cross-linked PGEs in terms of providing more charge carriers, Na^+ ions generally thought to be more mobile than the larger PF_6^- ions. The ionic conductivity climbed up with the increasing concentration of $NaPF_6$ in cross-linked PGEs, and then declined as the concentration of $NaPF_6$ surpassing 20 wt.% due to the increasingly strong interactions between polymer host and ionic liquids that interfere with ion transport. The highest ionic conductivity, 1.33×10^{-3} S cm^{-1}, was obtained for the sample with 20 wt.% $NaPF_6$. The behavior of the ionic conductivity at elevated temperature from 20 °C to 60 °C was consistent with the Arrhenius equation. The activation energies for cross-linked PGEs with different concentrations of 10 wt.%, 20 wt.% and 30 wt.% $NaPF_6$ are calculated to be 0.13 eV, 0.10 eV and 0.16 eV, respectively. These values also agree with the ionic conductivity trends where the low activation energy assists ion migration and improves the ionic conductivity. The electrochemical potential window for cross-linked PGEs was confirmed by cyclic voltammetry to be the range from -2.5 V to 2.5 V. The transference numbers, which varied from 0.90 to 0.96, demonstrate that cross-linked PGEs are predominantly ion-conducting electrolytes. Conclusively, this work enables the development of a mechanically robust PGE through cross-linking methodology with a working potential range sufficient to wide application of secondary batteries.

ACKNOWLEDGEMENT

The authors acknowledge the financial support from the Office of Naval Research Grant N00014-10-1-0677 and the support from Materials Science Program of University of Rochester. The assistance of Ms. Chris Pratt, Dr. Maria Abreu-Sepulveda, Dr. Patricia Taboada-Serrano and Rohit Puranik are gratefully acknowledged.

References

1. B. Oh, Y. K. Sun and D. W. Kim, *Bull. Korean Chem. Soc.,* 22 (2001) 1136.
2. M. Armand and J. M. Tarascon, *Nature,* 451 (2008) 652.
3. J. B. Goodenough and Y. Kim, *Chem. Mater.,* 22 (2010) 587.
4. D. E. Fenton, J. M. Parker and P. V. Wright, *Polymer,* 14 (1973) 589.
5. T. Sreekanth, M. J. Reedy, S. Ramalingaiah and U. V. S. Rao, *J. Power Sources,* 79 (1999) 105.
6. J. H. Shin, W. A. Henderson and S. Passerini, *Electrochem. Commun.,* 5 (2003) 1016.
7. N. A. Choudhur, S. Sampath and A. K. Shukla, *Energy Environ. Sci.,* 2 (2009) 55.
8. S. B. Ross-Murphy, *Formation, structure and properties of physical networks. In: PolymerNetworks: Principles of their Formation, Structure and Properties.,* R. F. T. Stepto, Chapman & Hall,(1998) Glasgow, U.K.
9. J. Y. Song, Y. Y. Wang and C. C. Wan, *J. Power Sources,* 77 (1999) 183.
10. J. M. Tarascon, A. S. Gozdz, C. Schmutz, F. Shokoohi and P. C. Warren, *Solid State Ionics,* 86 (1996) 49.
11. M. K. Song, Y. T. Kim, Y. T. Kim, B. W. Cho, B. N. Popov and H. W. Rhee, *J. Electrochem. Soc.,* 150 (2003) A439.

12. K. Murata, S. Izuchi and Y. Yoshihisa, *Electrochim. Acta*, 45 (2000) 1501.
13. S. Rajendran, O. Mahendran and R. Kannan, *J. Phys. Chem. Solids*, 63 (2002) 303.
14. E. Quartarone, P. Mustarelli and A. Magistris, *Solid State Ionics*, 110 (1998) 1.
15. J. Fang, J. Qiao, D. P. Wilkinson and J. Zhang J, *Electrochemical Polymer Electrolyte Membranes*, CRC Press, (2015) Boca Raton, Florida, U.S.
16. A. Laheaar, A. Janes and E. Lust, *Electrochim. Acta*, 82 (2012) 309.
17. D. Kumar and S. A. Hashmi, *J. Power Sources*, 195 (2010) 5101.
18. Q. Li, H. Chen, L. Lin, P. Li, Y. Qin, M. Li, B. He, L. Chu and Q. Tang, *J. Mater. Chem. A*, 1 (2013) 5326.
19. X. M. Qian, N. Y. Gu, Z. L. Cheng, X. R. Yang, E. K. Wang and S. J. Dong, *Electrochim. Acta*, 46 (2001) 1829.
20. A. Hayashi, K. Noi, A. Sakuda and M. Tatsumisago, *Nat. Commun.*, 3 (2012) 1843.
21. P. G. Pickup, *J. Chem. Soc.*, 86 86 (1990) 3631.
22. E. Barsoukov, J. R. Macdonald, *Impedance Spectroscopy: Theory, Experiment, and Applications*, John Wiley & Sons. Inc., (2005) Hoboken, New Jersey, U.S.
23. Y. Zhao, Y. G. Zhang, Z. Bakenov and P. Chen, *Solid State Ionics*, 234 (2013) 40.
24. M. M. Noor, M. H. Buraidah, M. A. Careem, S. R. Majid and A. K. Arof, *Electrochim. Acta*, 121 (2014) 159.
25. D. Kumar and S. A. Hashmi, *Solid State Ionics*, 181 (2010) 416.
26. M. Egashira, T. Asai, N. Yoshimoto and M. Morita M, *Electrochim. Acta*, 58 (2011) 95.
27. Z. Zhang, C. Zuo, Z. Liu, Y. Yu, Y. Zuo and Y. Song, *J. Power Sources*, 251 (2014) 470.
28. G. Li, Z, Li, P. Zhang, H. Zhang and Y. Wu, *Pure Appl. Chem.*, 80 (2008) 2553.
29. Y. Yang, Z. Chang, M. Li, X. Wang and Y. Wu, *Solid State Ionics*, 269 (2015) 1.
30. C. Sequeira, M. Plancha and L. Araujo, *J. Phys., IV.*, 4 (1994) C1.
31. S. J. Pas, M. D. Ingram, K. Funke, A. J. Hill, *Electrochim. Acta*, 50 (2005) 3955.
32. Q. Li, J. Wu, Z. Tang, Y. Xiao, M. Huang and J. Lin, *Electrochim. Acta*, 55 (2010) 2777.
33. M. Michae, M. Jacob, S. Prabaharan and S. Radhakrishna, *Solid State Ionics*, 98 (1997) 167.
34. L. E. Smart and E. A. Moore, *Solid State Chemistry: An Introduction*, CRC Press, (2005) Boca Raton, Florida, U.S.
35. C. Cao, W. Liu, L. Tan, X. Liao and L. Li, *Chem. Commun.*, 49 (2013) 11740.
36. K. Vignarooban, R. Kushagra, A. Elango, P. Badami, B. E. Mellander, X. Xu, T. G. Tucker, C. Nam and A. M. Kannan, *Int. J. Hydrogen Energy*, 41 (2016) 2829.
37. S. A. Hashmi and S. Chandra, *Mater. Sci. Eng., B*, 34 (1995) 18.
38. C. V. S. Reddy, A. K. Sharma and V. Rao, *J. Power Sources*, 114 (2003) 338.
39. P. B. Bhargav, V. M. Mohan, A. Sharma and V. N. Rao, *Curr. Appl. Phys.*, 9 (2009) 165.